

Document downloaded from:

<http://hdl.handle.net/10251/108468>

This paper must be cited as:

Orts Maiques, FJ.; Del Río García, AI.; Molina Puerto, J.; Bonastre Cano, JA.; Cases, F. (2018). Electrochemical treatment of real textile wastewater: Trichromy Procion HEXL. Journal of Electroanalytical Chemistry. 808:387-394. doi:10.1016/j.jelechem.2017.06.051



The final publication is available at

<https://doi.org/10.1016/j.jelechem.2017.06.051>

Copyright Elsevier

Additional Information

Electrochemical treatment of real textile wastewater: Trichromy PROCION HEXL®

*F. Orts, A.I. del Río, J. Molina, J. Bonastre, F. Cases**

*Departamento de Ingeniería Textil y Papelera, Escuela Politécnica Superior de Alcoy,
Universitat Politècnica de València. Plaza Ferrández y Carbonell, s/n, 03801, Alcoy,
Spain.*

*Corresponding author: F. Cases (fjcases@txp.upv.es)

ABSTRACT

The electrochemical treatment of wastewaters from the textile industry is a promising technique for not easily biodegradable compounds. This work is aimed at studying the electrochemical degradation of bifunctional reactive dyes after a real dyeing process. These are: Procion Yellow HELX®, Procion Crimson HELX® and Procion Navy HELX®, which are widely used in dyeing processes of cellulose fibers. Their structure is mainly characterized by the presence of two azo groups as chromophore group and two monochlorotriazinic groups as reactive groups. Electrolyses were carried out under galvanostatic conditions in an undivided electrolytic cell. Ti/SnO₂–Sb–Pt and stainless steel electrodes were used as anode and cathode, respectively. In all cases Na₂SO₄ was used as electrolyte without external addition of chloride.

The degree of degradation was evaluated by means of Total Organic Carbon (TOC) and Chemical Oxygen Demand (COD) measurements.

The decolourization kinetics and the presence of the intermediates generated due to of the electrochemical treatment were studied by High Performance Liquid Chromatography (HPLC) and these studies were also carried out with UV-Visible and Fourier Transform Infrared (FTIR) Spectroscopies.

In all cases, a decrease in TOC and COD, and a complete decolourization were obtained after the electrochemical treatment. AOS and COS data proved the presence of oxidised intermediates in solution after the electrolyses. These results suggest the possibility of reusing the treated water in several dyeing processes.

Keywords: Doped tin dioxide anodes; electrolysis; sulphate electrolyte; real textile wastewaters; Trychromy of bifunctional reactive dyes.

1. INTRODUCTION

The textile industry produces large amounts of wastewaters containing a high concentration of non-biodegradable organic compounds, mainly textile dyes. Nowadays, due to the environmental impact of this kind of wastewater, textile industries are showing a special interest in controlling this problem. In order to address this situation, a pre-treatment of this kind of wastewater is needed before discharge into natural effluents.

Reactive dyes are one of the most widely used in the textile industry. These dyes react chemically with the fibre giving rise to a covalent bond that permits excellent behaviour in washing and rubbing fastness tests. However, a certain percentage of un-fixed reactive dye generally remains in the residual dye bath as consequence of a competitive hydrolysis reaction that occurs during the dyeing process. This hydrolysed form of the dye (non-fixed dye), is responsible for the wastewater colour [1]. To diminish the amount of un-fixed dye, the use of bifunctional reactive dyes are of special interest because they have two reactive groups, and so, a two point fibre-dye bond. They have a fixation degree of around 80%, instead of 60% of the mono-functional dyes. However, the decrease of the amount of non-fixed dye in effluents is not enough to solve the problem of the wastewater colour because small amounts of a bifunctional dye are enough to produce intense coloration.

There are different methods to address the problem of colour and toxicity in textile dyeing effluent, such as: ozonation [2]; advanced oxidation processes [3-6]; enzymatic [7] or adsorption processes [8]. Moreover, electrochemical techniques have been found of special interest for textile wastewater remediation. Among others, their advantages are that this is a simple, clean and versatile technique where the electron is the only agent responsible for the degradation of the organic compounds [9]. Although electrochemical methods are quite efficient, coupling with other treatments such as biological methods generates a much more effective result. In recent years, electrochemical treatment as a solution to environmental problems has been studied in a number of journals [9-20]. Table 1 summarizes some examples of these studies. In most cases only one dye is chosen for the study. That dye usually has a simple molecular structure, a low concentration and the experimental conditions avoid the real conditions of the dye bath.

Table 1: Review of different chemical and electrochemical processes for the treatment of wastewater from textile dyeing.

Dye/Concentration	Electrolyte	Anode	Molecular structure	Removal	Reference
Reactive Black 5/ 20 mg L ⁻¹	HCl pH 4	TiO ₂ -Graphene oxide	Simple	80% decolouration	[3]
4-amino-3-hydroxy-2-p-tolylazo-naphthalene-1-sulfonic Acid/ 175 mg L ⁻¹	0.05 M Na ₂ SO ₄	Boron-doped diamond	Simple	92% TOC	[4]
Reactive Black 5/ 20 mg L ⁻¹	2 10 ⁻⁵ M Na ₂ SO ₄	Boron-doped diamond	Simple	82% TOC	[5]
Remazol Red/ 100 mg L ⁻¹	0.3-5.0 g L ⁻¹ NaCl	Anaerobic biofilm	Medium	> 90% COD	[6]
Reactive Blue 19/ 100 mg L ⁻¹	Potato dextrose at pH 6.8	Chemical oxidation by Endophytes	Medium-simple	90% decolouration	[7]
Reactive Yellow 160/ 100 mg L ⁻¹	4 g L ⁻¹ NaCl	PbO ₂ , SnO ₂	Simple	100% COD	[12]
Alphazurine/ 500 mg L ⁻¹	0.5 M Na ₂ SO ₄	PbO ₂	Simple	90% COD	[12]
Methyl Red/ 100 mg L ⁻¹	H ₂ SO ₄ pH 3	PbO ₂	Simple	90% COD	[12]
Reactive Orange 16/ 85 mg L ⁻¹	0.1 M Na ₂ SO ₄	β-PbO ₂	Simple	90% TOC	[12]
Methyl Green/ 300 mg L ⁻¹	0.5 M H ₂ SO ₄	PbO ₂	Simple	82% TOC	[12]
Mixture of real dyeing textile effluents	170 mg L ⁻¹ Cl ⁻ + 19 mg L ⁻¹ SO ₄ ²⁻	Boron-doped diamond	Unknown	90% COD	[17]

In environmental electrochemistry, operating conditions, the composition of the electrolyte, the reactor design and electrode material are the main factors that must be taken into account. The type of electrode directly influences in the nature of the

products formed during and after the electrolysis. Dimensionally Stable Anodes (DSA®) constitute by far one of the most attractive materials for electrochemical treatment. For this reason, in the present work, Ti/SnO₂-Sb-Pt has been chosen as anode for the ~~oxide-reduction~~ electrochemical treatment of textile wastewaters aiming at decontamination. In previous studies carried out by this research team, it has been proven that Ti/SnO₂-Sb-Pt electrodes are efficient in the electrochemical treatment of solutions containing mono-functional and bifunctional reactive azo dyes [21-22]. It has been shown that these electrodes present high chemical and electrochemical stability, high electrical conductivity and high oxygen evolution over-potential. Moreover, the introduction of small amounts of platinum in the coating produces an increase in the service life of several orders of magnitude [23].

In particular, the present research studies the electrochemical degradation of products obtained after the dyeing process of cotton fabrics with three bifunctional reactive dyes. These dyes correspond to the HEXL trichromy, and they are Procion Yellow HEXL®, Procion Crimson HEXL® and Procion Navy HEXL®. They have two monochlorotriazinic groups as reactive groups and they also present two azo groups (—N=N—) as chromophore groups [24] (Figure 1 and Table 2). Reactive dyes have been the most significant innovation in textile dyeing technology in the 20th century. After dyeing, the dye that remains in the solution has the —Cl substituents exchanged, in the chlorotriazinic group, by —OH as consequences of the hydrolysis. The extent to which dye hydrolysis takes place in competition with dye-fibre reaction varies quite markedly within the range 10-40% depending on the system in question. The most successful approach to addressing this issue has been the development of dyes with more than one fibre-reactive group in the molecule, which statistically improves the chances of dye-fibre bond formation [25].

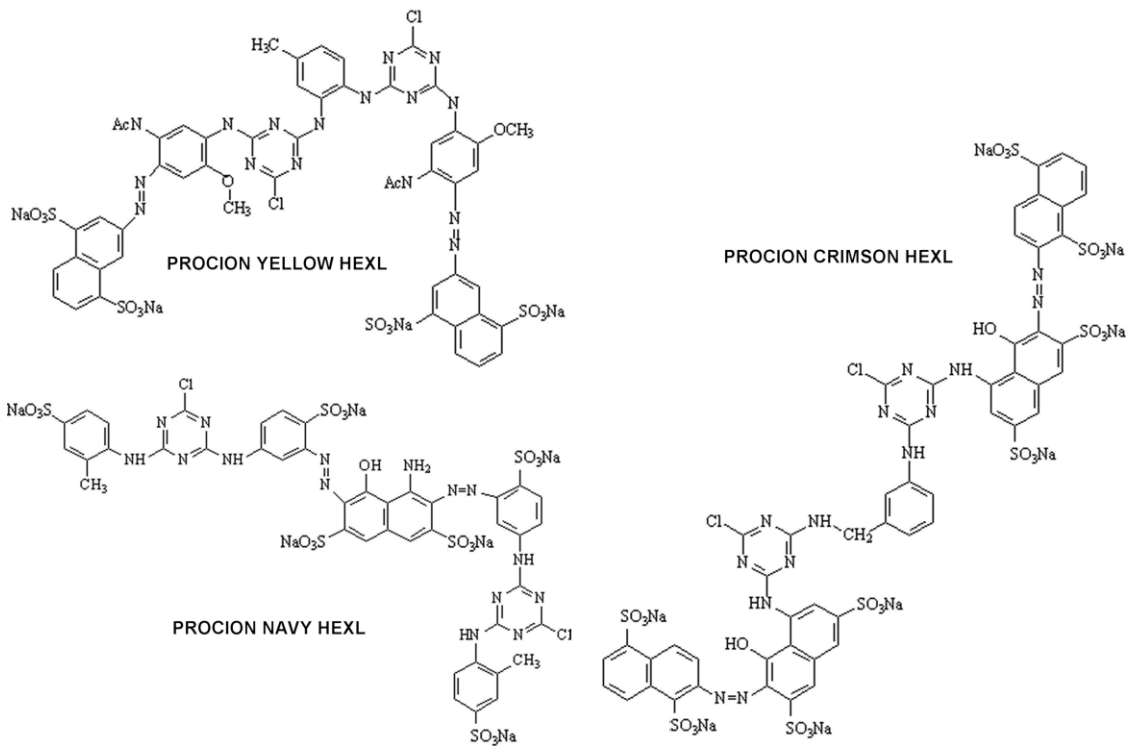


Figure 1. Molecular structure of the three dyes of the HEXL Trichromy.

The main objective of this current work is to study the degree of electrochemical degradation of the different dyes, mixed to obtain the trichromy, which form part of a textile effluent under real conditions and the possible interactions between them. Moreover, in the development of the research, special attention has been paid to the color removal of reactive dye-containing solutions which permits the reuse of the treated water. Thus, reuse of the effluent produces useful materials (for example reusing not only water but also the electrolytes used in the dye). All these were carried out using Na₂SO₄ as electrolyte without adding NaCl in the reaction medium. Thus, indirect chemical oxidation by oxidation products of chloride is not relevant. Sulphate is an inert supporting electrolyte and it does not produce any reactive species during the electrolysis, except under special conditions where it may generate persulphate. Another of the hypotheses formulated in this work is whether with these experimental conditions (developed anodes, cell configuration, electrolyte media, among others) it is possible to decolorize and degrade, not only, complex chemical structure of dyes (bi-functional and di-azo), but also solutions with a mix of three of these dyes (Trichromy). All these after a real dyeing process. Finally, it is important to check the stability of the anodes developed, which are less expensive than others used in the bibliography.

Table 2. Description of the selected reactive dyes.

Abbr	Comercial Name	C.I. Name	Chromophore	Reactive group	λ_{max} (nm)
PY	Procion Yellow HEXL®	Reactive Yellow 138:1	Diazo	Monoclorotriazinic	420
PC	Procion Crimson HEXL®	Reactive Red 231	Diazo	Monoclorotriazinic	549
PN	Procion Navy HEXL®	Non registered	Diazo	Monoclorotriazinic	610

2. MATERIALS AND METHODS

2.1 Dyes and dyeing reagents

Dyes used in all experiments were kindly supplied by Dystar (Singapore) and used as received without further purification. The rest of the chemical products used in the dyeing process (NaOH , H_2O_2 and Na_2SO_4) were supplied by Merck and Fluka (analysis quality). Distilled water was used for the preparation of all solutions.

In all cases the electrolyte used was Na_2SO_4 in a concentration of 45.00 g L^{-1} and the specific conductivity of dye solutions were 42.0 mS cm^{-1} . The pH before dyeing was 7.0 and after dyeing was between 10.8 and 11.0. Dye solutions before dyeing used were:

PY solution: Procion Yellow HEXL® with a concentration of 1.50 g L^{-1} .

PC solution: Procion Crimson HEXL® with a concentration of 1.50 g L^{-1} .

PN solution: Procion Navy HEXL® with a concentration of 1.50 g L^{-1} .

TRICHRAMY solution: a mix of the three dyes with a concentration of each one of 0.50 g L^{-1} .

2.2 Dyeing process

For each of the dye solutions described in the previous paragraph, seven samples were prepared, each of which contained 0.125 L of dye solution and 10.00 g of fabric 100 % semi-whitened cotton (previously washed in a solution of H_2O_2 and NaOH). The liquor ratio was 1:12.5 and the ratio of dyestuff in relation to the fabric was $1.87 \text{ g dye/g woven}$.

To accomplish the dyeing process reproducing the same conditions of the dyeing process used in the facilities of the factory, with a consumption of a small amount of reactive and fabrics, the samples were inserted in the sample holders of a RED-TEST

(UNGOLINI model RT-P) with its corresponding bath of dye. Sample holders are pipes of stainless steel of 40 mm of diameter and 160 mm of height with maximum capacity of 180 ml of bath. These pipes are placed in the equipment under the following conditions:

- Initial temperature: 15.0 °C.
- Gradient of temperature: 1.5 °C min⁻¹.
- Final temperature: 80.0 °C (± 2.0 °C).

The dyeing process took two hours from the start to finish. During the dyeing there is a constant rotation of the backbone of the equipment where the pipes are placed to obtain a good equalization of the dyes. The NaOH solution was added after 60 minutes.

The dyeing processes were done in the facilities of the Texcoy Company (Spain).

2.3 Electrolysis

The electrolyses of the alkaline aqueous solutions containing the hydrolysed dyes obtained after the dyeing process were carried out in an undivided filter press reactor as the one shown in figure 2 [22]. Redox process at 125 mA cm⁻² was chosen as the best operation conditions to produce the fastest decolouration of the solution and the greatest degradation of dyes under these experimental conditions [21-22, 26]. Moreover, in previous works where current densities of 125 and 250 mA cm⁻² have been checked, the one with the highest average current efficiency and the lowest energy consumption was 125 mA cm⁻². Ti/SnO₂-Sb-Pt electrodes with mesh geometry were used as anode. These electrodes were prepared following a standard thermal decomposition method of the salt precursor on a titanium substrate [26]. Titanium mesh with a geometrical active area of 48,8 cm⁻² (10.0 cm X 8.0 cm) was first pre-treated in order to eliminate the superficial layer of TiO₂ (electric semiconductor). Moreover, a higher roughness was obtained that allowed an increase in the adherence of the deposits to the support. Later, the titanium supports were degreased with acetone using ultrasounds for 10 min and etched for 1 h in a boiling solution of oxalic acid (10%). After that, the supports were rinsed with ultrapure water and the precursor solution was brushed onto the Ti plate. This precursor solution contained 10% SnCl₄-5H₂O (provided by Aldrich) + 1% SbCl₃ (purchased from Fluka) + 0.252% H₂PtCl₆-6H₂O (supplied by Merck) dissolved in a mixture of ethanol (provided by Panreac) + HCl (supplied by Merck). Afterwards, the electrodes were introduced in an oven at 400°

C for 10 min. With this thermal treatment, the decomposition of the salt and the formation of the metal oxide take place. This process was repeated up to a weight increase of about 2 mg cm^{-2} . Finally, a thermal treatment at 600°C was applied for 1 h.

A stainless steel electrode of $11.0 \text{ cm} \times 9.5 \text{ cm}$ ($\text{Cr } 18\text{-}19\%$ y $\text{Ni } 8.5\text{-}9\%$) was used as cathode. This was previously pre-treated by means of mechanical, chemical and electrochemical processes in order to eliminate any kind of surface contamination. Figure 2 shows a picture of the undivided filter press reactor used in the electrolyses experiments. The volume of the dye solution treated was 0.420 L in all cases, the operation temperature reached 40° C and the flow rate was 5.600 L min^{-1} . All the experiments were carried out under galvanostatic conditions with a power supply (Grelco GVD310 0-30Vcc / 0-10 A).

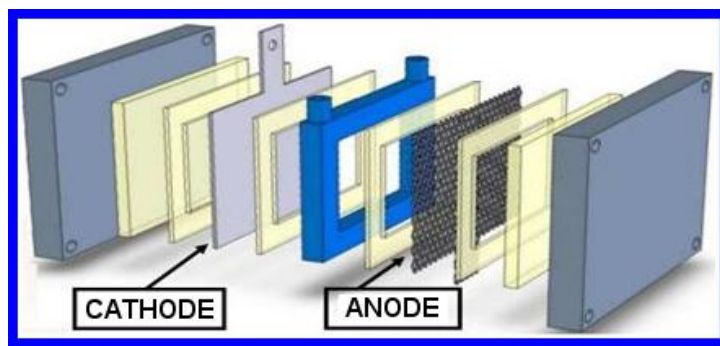


Figure 2. Undivided filter press reactor

2.4 Analysis and Instruments

Different samples were collected during the electrolyses. They were used to perform TOC and COD measurements. The evaluation of these parameters allowed the degree of degradation to be followed closely.

A Shimadzu TOC-VCSN analyser was used to obtain TOC values. The measurement parameters were: Operated temperature: 1193 K; injection volume of sample: $20.0 \mu\text{L}$; air flow rate: 0.150 L min^{-1} (free of CO_2). Samples were diluted to bring their concentration within the operating range of the apparatus. A Spectroquant analyser was used to obtain COD values. The method used for these measurements is analogous to EPA 410.4, US Standard Methods 5220 D and ISO 15705.

A Hitachi Lachrom-Elite Chromatographic System equipped with diode array detector was used to do chromatographic analyses performed by means of High Performance Liquid Chromatography (HPLC). The measurements parameters were: Column: Lichrospher 100 RP-18 C with $5.00 \mu\text{m}$ packing using a similar method to that in EN

14362-2:2003/A; mobile phase composition: methanol (eluent A) / aqueous buffer solution $\text{KH}_2\text{PO}_4\text{-Na}_2\text{HPO}_4$ (eluent B) with pH 6.9; flow rate: 1 mL min⁻¹; temperature: 298 K; injection volume: 20.0 µL. At the beginning of the chromatographic separations, the gradient elution consisted of 100 % aqueous buffer and it was progressively modified to 100% methanol within 20 min. The detection wavelength was set at 420, 549 and 610 nm for Procion Yellow®, Procion Crimson® and Procion Navy®, respectively. These are the wavelengths at which the azo groups of each dye absorb.

UV-Visible spectra were also obtained with this system. This was made possible by changing the column for a tubular piece (without any packing inside). This allowed the sample to flow to the detector with low volume consumption.

The FTIR-ATR spectra were recorded with a FTIR NICOLET 6700 spectrophotometer equipped with a horizontal ATR device, in which the bottom of the surface prism (ZnSe) serves as the cavity for aqueous samples. The subtraction of the background signal (aqueous solution of Na_2SO_4 and NaOH under the same conditions as the samples obtained after dyeing and free of dye) was required to obtain the spectra of the different samples. The spectra were collected at 8 cm⁻¹ resolution as a result of an average of 400 scans.

2.5 Parameters evaluated

In this study some parameters have been used which provide details of, for example, the variations of the sample composition which could affect the toxicity/biodegradability of the solution. This is the case of the Average Oxidation State (AOS) [27-29]. This parameter indicates the variations of the sample composition, which could affect the toxicity/biodegradability of the solution. This parameter is calculated using the following expression:

$$AOS = 4 \frac{(TOC_t - COD_t)}{TOC_t} \quad (1)$$

To obtain information on the degree of oxidation of the organic matter contained in samples collected throughout the treatment, the Carbon Oxidation State (COS) must be calculated [30]. This parameter indicates the degree of oxidation of the organic matter contained in samples collected throughout the treatment. It uses the initial organic carbon as a reference and it is calculated according to the following expression:

$$COS = 4 \frac{(TOC_0 - COD_t)}{TOC_0} \quad (2)$$

In AOS equation as well as in COS one, both TOC value and COD values are expressed in molar units.

To obtain the overall efficiency of the process, the parameter that must be calculated is the Average Current Efficiency (ACE) which evaluated the fraction of the applied current that is used to diminish the initial COD by a certain percentage [31-36]. This parameter indicates the fraction of the applied current, which is used to diminish the initial COD in a certain percentage. In other words, this parameter gives an idea of the overall efficiency of the process and it is determined using the following expression:

$$ACE = \frac{COD_0 - COD_t}{8 \cdot I \cdot t} \cdot F \cdot V \cdot 100 \quad (3)$$

Where COD_0 and COD_t are the initial COD and the COD in a selected loaded charge during electrolysis ($\text{g O}_2 \text{ L}^{-1}$), respectively, F is the Faraday constant (96487 C mol^{-1}), V is the volume of the wastewater (L), I is the applied current (A), t is the time of electrolysis (s) and 8 is the equivalent weight of oxygen.

3. RESULTS AND DISCUSSION

3.1. Kinetics results and operating costs.

Decolourization during the electrolyses was monitored by means of HPLC technique. With this aim in mind, the evolution of the dye concentration during the electrolysis of all the species that contribute to the color of the solution was measured according to the normalized chromatographic area (S/S_0) of the peak observed (where S_0 is the area of the peak when $Q = 0.00 \text{ Ah L}^{-1}$). To obtain the chromatographic peaks, the detector wavelength was set at: 420 nm for Procion Yellow HEXL®, 549 nm for Procion Crimson HEXL® and 610 nm for Procion Navy HEXL®. This was possible considering that the dye concentrations of the species that contribute to the colour are directly related to the chromatographic areas. Figures 3 a-c show the evolution of the chromatographic profile during the electrolysis of the three dye solutions. The variation of the concentration of the species that contribute to the colour can be evaluated by

plotting the evolution of $\ln(S/S_0)$ versus the loaded charge ($Ah L^{-1}$), as shown in Figure 3-d. Under the experimental conditions described above, all the electrolyses followed a pseudo first order kinetics with respect to dye concentration, as could be deduced from the fit of the profiles.

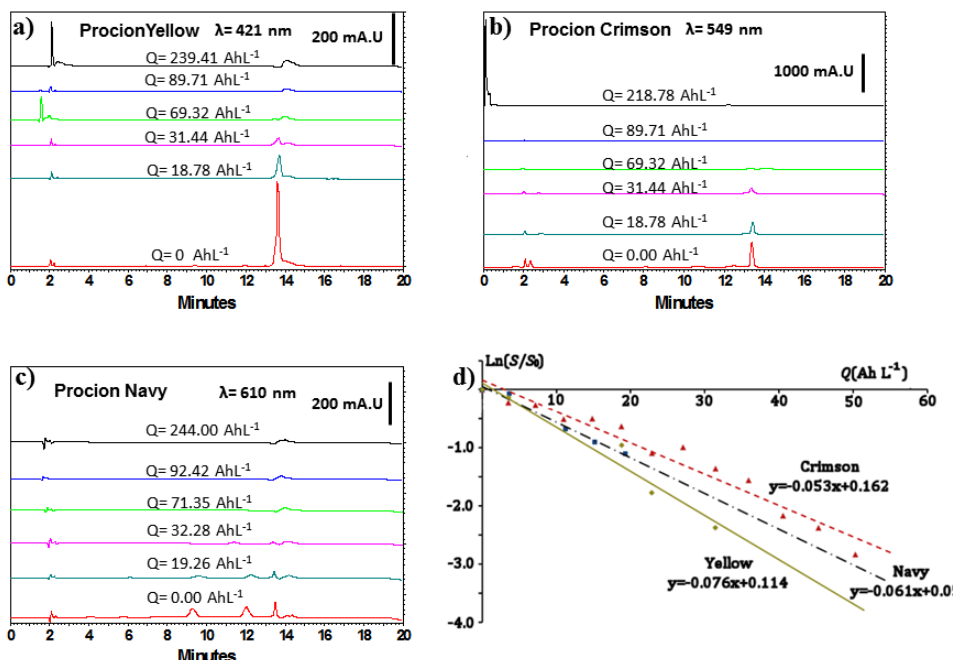


Figure 3. Evolution of the chromatographic profile during the electrolysis of the solutions of: a) Procion Yellow®; b) Procion Crimson® and c) Procion Navy®. d) Logarithm of the normalised chromatographic area versus loaded charge $Q (Ah L^{-1})$ of samples obtained during the redox process at 125 mA cm^{-2} . The initial solutions were the three hydrolysed dyes obtained after the dyeing processes.

Table 3 shows a compilation of the kinetics results obtained from the linear regression analysis for the plots $\ln(S/S_0)$ vs. $Q (Ah L^{-1})$ (Figure 3). All the decolourization kinetics rates are very similar, between 0.05 to $0.08 A^{-1} h^{-1} L$. Table 3 also shows the Q needed to obtain complete decolourization (assuming a decrease in the dye concentration of 99 per cent as complete decolourization), which occur in the range 60.00 - $90.00 Ah L^{-1}$. In the next section, the higher value of this range ($90.00 Ah L^{-1}$) is selected to choose the samples which are practically decolourized and compare their TOC and COD values at the same Q .

These results mean that the treated water in several dyeing processes could be reused. Interim studies made by this research group show that a new dyeing process allows 70% of the dyeing water to be saved and leads to a considerable reduction of effluent salinity and dumping costs.

Table 3. Kinetics analyses and energy consumption per order obtained for all the electrolyses: decolourization kinetics rate ($A^{-1} h^{-1} L$), specific charge ($A \text{ hL}^{-1}$) for a complete decolourization (99 per cent) and energy consumption per order ($kWh L^{-1}$).

DYE SOLUTION	λ (nm)	k_{ap} ($A^{-1} h^{-1} L$)	Q_{dec} ($Ah L^{-1}$)	EEO ($kWh L^{-1}$)
PROCIÓN YELLOW HEXL®	420	0.076	62.18	0.22
PROCIÓN CRIMSON HEXL®	549	0.054	88.40	0.74
PROCIÓN NAVY HEXL®	610	0.061	75.81	0.64

Apart from the kinetics analysis, one of the most important parameters affecting the performance of an electrochemical system is the operating costs. With this purpose in mind, the electrical energy consumption per order (EEO) was calculated in all cases. The calculus of EEO was chosen according to the report of Bolton et al [37], considering that the concentration of pollutants in all cases were low. This parameter is defined as the electrical energy in kilowatt-hour (kWh) required to degrade a contaminant by a unit of volume of contaminated water or air. The corresponding equation is the following:

$$EEO = \frac{P \cdot t}{V \cdot \log\left(\frac{A_i}{A_f}\right)} \quad (4)$$

Where: P is the electric power (kW), t is the time of electrolysis (h), V is the volume treated (L), A_i and A_f are the initial and final area of the chromatographic peak associated to the pollutant of interest.

In the present study, the values of the dye concentration ($g L^{-1}$) remaining in solution after electrolyses were difficult to measure since the percentages of dye degradation were very high. However, the chromatographic peak associated with the chromophore group of the dye could be considered. This is because the area of the peak is directly proportional to the concentration of dye whose chromophore group has not been degraded yet, as previously mentioned. Therefore, the area of this peak was used in

calculations instead of concentration. The values obtained have been included in Table 3.

3.2. TOC and COD measurements

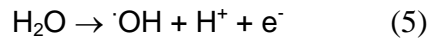
Table 4 shows the results corresponding to TOC and COD removal as well as the values of AOS, COS and ACE measured from samples obtained at the beginning and at the end of electrolyses, with a Q of 240.00 Ah L⁻¹ approximately. This value of total applied specific charge was selected to compare the final samples when parameters such as TOC and COD were practically invariable. In the table, intermediate values obtained at a loaded charge near to 90.00 Ah L⁻¹ are also shown. It was verified across the chromatographic analyses that for these values of loaded charge complete decolourization was obtained.

Table 4. Results of TOC removal, COD removal, values of AOS, COS and ACE of samples obtained at different loaded charges in the electrolysis processes.

DYE SOLUTION	Q (A.h L ⁻¹)	TOC (mgL ⁻¹)	TOC REMOVAL (%)	COD (mg L ⁻¹)	COD REMOVAL (%)	AOS	ΔAOS	COS	ΔCOS	ACE (%)
P. YELLOW	0.00	271.55	-	882.67	-	-0.88	-	-0.88	-	-
	89.71	232.50	14.38	648.00	26.59	-0.18	0.70	-0.15	0.72	1.11
	239.41	170.25	37.30	520.00	41.09	-0.58	0.29	-0.36	0.51	0.70
P. CRIMSON	0.00	422.00	-	1768.00	-	-2.28	-	-2.28	-	-
	89.71	388.35	7.97	1319.33	25.38	-1.10	1.19	-1.01	1.28	2.12
	218.78	338.80	19.72	986.00	44.23	-0.37	1.92	-0.29	1.99	1.63
P. NAVY	0.00	351.45	-	1312.00	-	-1.60	-	-1.60	-	-
	92.42	293.65	16.45	826.00	37.04	-0.22	1.38	-0.18	1.42	2.24
	244.00	206.20	41.33	533.33	59.35	0.12	1.72	0.07	1.67	1.50
TRICHRONY	0.00	346.35	-	1192.00	-	-1.16	-	-1.16	-	-
	92.42	330.10	4.69	896.50	24.79	-0.07	1.09	-0.07	1.09	1.36
	247.39	252.70	27.04	682.67	42.73	-0.05	1.11	-0.04	1.12	0.97

The evolution of COD removal during the electrolysis was quite similar in all dye solutions studied. TOC removal showed some differences. Procion Crimson HEXL® solutions have the lowest value of TOC removal and, as consequence of this, the values of the trichromy are lower too. As Table 3 shows, Procion Crimson® solutions needed the higher loaded charge for decoloring and its kinetics rate is the lowest. Nevertheless, in all cases, values of TOC and COD removal at the end of the electrolysis are noticeable. This feature could be explained because anodes coated with SnO₂ are known as “non-active” electrodes, so they do not participate in the

oxidation; they only provide adsorption sites for OH radicals generated as a result of water lysis (Reaction 5) [16 and references therein]:



These radicals are highly oxidative and facilitate the degradation of organic matter.

In all cases, the percentage of COD removed was greater than that of TOC. Moreover, changes in AOS values are related to changes in solution composition as a consequence of the electrochemical treatment. In all cases, an increase in the AOS values was observed. Therefore, after all the electrolyses, the organic matter that remains in solution have more positive oxidation states [21] and these oxidised intermediates should be stable in solution as TOC removal results indicated. In other words, the products of electrolysis have a higher oxidation state than dyes before electrolysis. This behaviour was confirmed by the increase of COS values associated with the processes.

Values of ACE (%) are shown in Table 4. In all cases, a decrease of ACE percentage during the electrolysis time occurs (see values around 90.00 Ah L^{-1} and 240.00 Ah L^{-1} of loaded charge). This could be explained by the fact that initially the main reactions are the degradation of the chromophores and the reactive groups of the dye molecules (as will be pointed out in the next section) and as their concentration decreases, more complex degradation reactions and, mainly, the electrolysis of the water are given increasing lengths of time and thus efficiency decreases. According to other published studies, simpler molecular structures give higher ACE (%) values. The present work deals with the electrochemical degradation of three reactive dyes whose molecular weight is far higher than other dyes commonly studied, and moreover with no presence of an inorganic mediator such as “active chlorine”. Additionally, it should be taken into account that the dyes studied in this work are protected by patents so their purity is unknown. Among other reasons, this is because the solutions are obtained after a real dyeing process of cotton fabrics that provide non-controlled solutes.

3.3 Spectroscopic results

Figure 4 shows the evolution of the UV-Vis spectra of the trichromy solution with the loaded charge during the electrolysis. The more important features that can be observed are:

- The bands centered at 420 nm, 549 nm and 610 nm, which are associated with the chromophores groups of the Procion Yellow HEXL®, Procion Crimson

HEXL® and Procion Navy HEXL® respectively, completely disappear at the beginning of the electrolysis. So, a complete decolourization takes place.

- The band centered at 280 nm, which is associated with the presence of triazinic groups [38], completely disappears at the beginning of the electrolysis.
- The band centered at 230 nm, which is associated with a $\pi \rightarrow \pi^*$ transition of the benzenic rings [39-42], does not disappear indicating that these molecular structures remain as products of the electrolysis.
- At the end of the electrolysis a new band appears at 210 nm, typically associated with $\pi \rightarrow \pi^*$ transitions of highly oxidised groups, such as carbonyl [38].

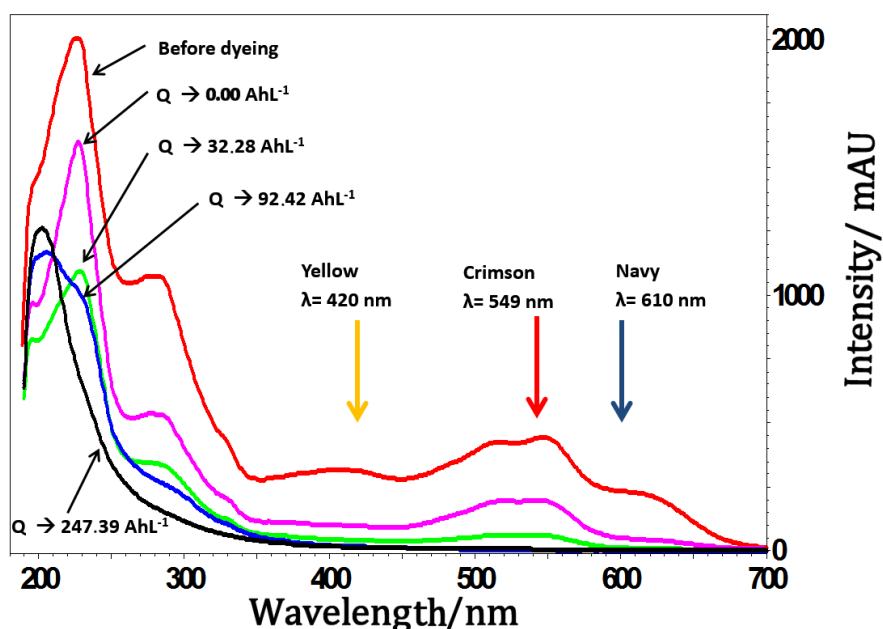


Figure 4. Evolution of the UV-Vis spectra of the trichromy solution with the loaded charge during the electrolysis. The bands related to the three chromophores are centred at 420 nm, 549 nm and 610 nm, approximately.

Figure 5 shows the FTIR spectra of the trichromy solutions before and after electrolysis.

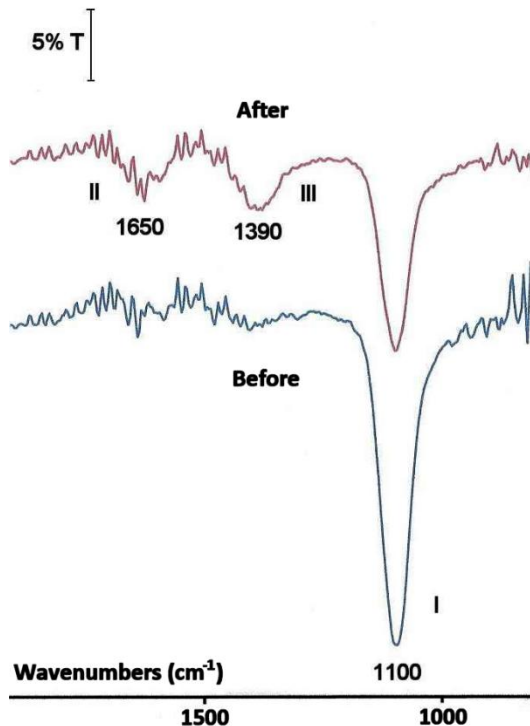


Figure 5. FTIR spectra of the trichromy solution before and after electrolysis.

In the FTIR spectrum of the solution used before electrolysis, a band (Band I) centered at 1100 cm^{-1} can be clearly observed. This band diminishes after the electrolysis and at the same time two bands centered around 1650 cm^{-1} (Band II) and 1390 cm^{-1} (band III) appeared. These two bands are present in the spectrum before electrolysis but their intensity is lower. If we bear in mind the redox treatment of the solution and the results obtained by means of UV-Vis spectroscopy, it is possible to explain the above-mentioned bands. Band I may be associated with the stretching C-O vibration of the hydroxyl groups [43] or to the symmetric stretching vibration of C - O of the ethers alkyl-aryl [44], both present in the original molecules. The above mentioned band diminishes after the electrolysis at the same time as band II increases. Band II may be associated to the oxidation of the hydroxyl and ether groups, among others, giving, for example, quinoid structures (that are in presence of hydroxyl or amine groups) [44] or carbonyl groups in aromatic ring [43]. The appearance of bending vibrations of N-H as a product of the reduction the azo group could not be discarded. Both deductions, the appearance of oxidised groups and the elimination of the chromophore group, were made when the UV-Vis spectra were analysed. In addition, it is known that as a consequence of the electrolysis EOP and EOC present a significant increase of 1.1, in both cases.

Nevertheless, even when lower intensity was applied, band II was already observed in the spectrum of the original solution. Therefore, it is not possible to reject the possibility that an overlap exists between the bands associated to: vibration modes of the aromatic ring [45], imine groups (C=N-) presents in the tautomeric form of the azo group [44] and secondary amides where the substituent of the N is an aromatic ring [44]. All of which are present in the spectrum before electrolysis.

Band III could be associated to the presence of para-disubstituted benzenes or to C=C vibration of naphthalenic rings [44]. This band is weak in the spectrum before electrolysis and increases after electrolysis.

The partial transformation of the molecule as a consequence of the electrolysis (deduced by the decrease of TOC and COD, 27 % and 43 %, respectively) and the band centred at 230 nm observed in the spectrum UV-Vis (associated with benzenic rings) whose intensity did not change allowed to affirm that the partial opening of the naphthalenic rings plays an important role in the increase of the band after the electrolysis since benzenic compounds were formed and they are more stable in the experimental conditions.

CONCLUSIONS

Electrolyses of real dyestuff wastewaters were carried out in a filter-press cell in galvanostatic conditions and using Ti/SnO₂-Sb-Pt electrode as anode and stainless steel electrode as cathode. Aqueous solutions obtained after dye processes of cotton fabrics of hydrolyzed dyes of the Trychromy HEXL were used. The electrolyte used was Na₂SO₄ (without external addition of chloride).

Complete decolourization was observed in all cases and there was no noticeable difference in the loaded charge needed for the decolourization in solution with a single dye or with the trichromy (around 90.00 Ah L⁻¹ under the present experimental conditions). Therefore, the nature of the chromophore and the similar molecular structure seems to be the characteristic that mainly influences the decolourization mechanism. The decolourization process followed a pseudo-first order kinetics.

The removal of TOC and COD (higher in the last case), the increase of EOP and EOC and the evolution of the UV-Vis and ATR-FTIR spectra, strongly suggested that at the start of the electrolysis the main reactions are the degradation of the chromophores and the reactive groups of dye. The presence, after the electrolysis, of stable intermediates was confirmed. These contain, in their molecular structure, aromatic carbonyl groups and benzenic rings with quinoids structure partially formed during the

partial opening of the original naphthalenic rings.

These results indicate that the electrochemical technique described can be considered an ecofriendly method for the treatment and reuse of dyeing effluents.

ACKNOWLEDGMENT

The authors wish to thank the Spanish Agencia Estatal de Investigación (AEI) and European Union (FEDER funds) for the financial support (contract MAT2016-77742-C2-1-P). A.I. del Río is grateful to the Spanish Ministerio de Ciencia y Tecnología for her FPI fellowship. J. Molina is grateful to the Conselleria d'Educació, Formació i Ocupació (Generalitat Valenciana) for the Programa VALi+D Postdoctoral Fellowship (APOSTD/2013/056). The authors wish to acknowledge to the Texcoy S.L. company (Spain) where the dyeing processes were done and Tim Vickers for help with the English revision.

REFERENCES

- [1] Integrated Pollution Prevention and Control (IPPC). Reference Document on Best Available Techniques for the Textile Industry. July 2003. European Commission.
- [2] X.B. Zhang, W.Y. Dong, W. Yang, Decolorization efficiency and kinetics of typical reactive azo dye RR2 in the homogeneous Fe(II) catalyzed ozonation process. *Chemical Engineering Journal* 233 (2013) 14-23.
<http://dx.doi.org/10.1016/j.cej.2013.07.098>
- [3] A.B.S. Nossol, S.M.C. Rosa, E. Nossol, A.J.G. Zarbin, P. Peralta-Zamora, Photocatalytic degradation of dye over graphene-TiO₂ nanocomposite. *Química Nova* 39 (2016) 686-690.
<http://dx.doi.org/10.5935/0100-4042.20160081>
- [4] L. Labiad, M.A. Oturan, M. Panizza, N.B. Hamadi, S. Ammar, Complete removal of AHPS synthetic dye from water using new electro-fenton oxidation catalyzed by natural pyrite as heterogeneous. *Journal of Hazardous Materials* 297 (2015) 34-41.
<http://dx.doi.org/10.1016/j.jhazmat.2015.04.062>
- [5] V.M. Vasconcelos, C. Ponce-de-León, J.L. Nava, M.R.V. Lanza, Electrochemical degradation of RB-5 dye by anodic oxidation, electro-Fenton and by combining anodic oxidation-electro-Fenton in a filter-press flow cell. *Journal of Electroanalytical Chemistry* 765 (2016) 179-187.
<http://dx.doi.org/10.1016/j.jelechem.2015.07.040>
- [6] M. Punzi, A. Anbalagan, R.A. Börner, B.M. Svensson, M. Jonstrup, B. Mattiasson, Degradation of a textile azo dye using biological treatment followed

by photo-Fenton oxidation: Evaluation of toxicity and microbial community structure. Chemical Engineering Journal 270 (2015) 290-299.
<http://dx.doi.org/10.1016/j.cej.2015.02.042>

- [7] L.M.C. Bulla, J.C. Polonio, A.L.B. Portela-Castro, V. Kava, J.L. Azevedo, J.A. Pamphile, Activity of the endophytic fungi Phlebia sp. and Paecilomyces formosus in decolourisation and the reduction of reactive dyes' cytotoxicity in fish erythrocytes. Environmental Monitoring and Assessment 189:88 (2017) 1-11.
<http://dx.doi.org/10.1007/s10661-017-5790-0>
- [8] A. Hethnawi, N.N. Nassar, A.D. Manasrah, G. Vitale, Polyethylenimine-functionalized pyroxene nanoparticles embedded on Diatomite for adsorptive removal of dye from textile wastewater in a fixed-bed column. Chemical Engineering Journal 320 (2017) 389-404.
<http://doi.org/10.1016/j.cej.2017.03.057>
- [9] E. Brillas, C.A. Martínez-Huitl, Decontamination of wastewaters containing synthetic organic dyes by electrochemical methods. An updated review. Applied Catalysis B: Environmental 166-167 (2015) 603-643.
<http://doi.org/10.1016/j.apcatb.2014.11.016>
- [10] E. Brillas, P.L. Cabot, J. Casado, *Chemical Degradation Methods for Wastes and Pollutants Environmental and Industrial Applications*. 1st Ed. New York: Ediciones M.A. Tarr. Marcel Dekker, 2003, p.235–304. ISBN: 978-0824743079.
- [11] C.A. Martínez-Huitl, M.A. Rodrigo, I. Sirés, O. Scialdone, Single and Coupled Electrochemical Processes and Reactors for the Abatement of Organic Water Pollutants: A Critical Review. Chemical Reviews 115 (2015) 13362-13407.
10.1021/acs.chemrev.5b00361
- [12] A.N. Subba Rao, V.T. Venkatarangaiah, Metal oxide-coated anodes in wastewater treatment. Environmental Science and Pollution Research 21 (2014) 3197-3217.
10.1007/s11356-013-2313-6
- [13] I. Sirés, E. Brillas, M.A. Oturan M. A. Rodrigo, M. Panizza, Electrochemical advanced oxidation processes: today and tomorrow. A review. Environmental Science and Pollution Research 21 (2014) 8336-8367.
10.1007/s11356-014-2783-1
- [14] M. Panizza, G. Cerisola, Direct and mediated anodic oxidation of organic pollutants. Chemical Reviews 109, 2009, 6541-6569.
10.1021/cr9001319
- [15] C.A. Martínez-Huitl, S. Ferro, Electrochemical oxidation of organic pollutants for the wastewater treatment: Direct and indirect processes. Chemical Society Reviews 35, 2006, 1324-1340.
10.1039/B517632H
- [16] D.A. Jadhav, S.G. Ray, M.M. Ghangrekar, Third generation in bio-electrochemical system research – A systematic review on mechanisms for

recovery of valuable by-products from wastewater. Renewable and Sustainable Energy Reviews 76 (2017) 1022-1031
<http://doi.org/10.1016/j.rser.2017.03.096>

- [17] N. Abdessamad, H. Akroud, L. Bousselmi, Anodic oxidation of textile wastewaters on boron-doped diamond electrodes. Environmental Technology (United Kingdom) 36 (2015) 3201-3209.
<http://doi.org/10.1080/09593330.2015.1056235>
- [18] L. Pang, H. Wang, Z.Y. Bian, Treatment of methyl orange dye wastewater by cooperative electrochemical oxidation in anodic-cathodic compartment. Water Science and Technology 67 (2013) 521-526.
<http://doi.org/10.2166/wst.2012.589>
- [19] B.P. Chaplin, Critical review of electrochemical advanced oxidation processes for water treatment applications. Environmental Sciences: Processes and Impacts 16 (2014) 1182-1203.
<http://doi.org/10.1039/c3em00679d>
- [20] S.O. Ganiyu, E.D. Van Hullebusch, M. Cretin, G. Esposito, M.A. Oturan, Coupling of membrane filtration and advanced oxidation processes for removal of pharmaceutical residues: A critical review. Separation and Purification Technology 156 (2015) 891-914.
<http://doi.org/10.1016/j.seppur.2015.09.059>
- [21] A.I. del Río, J. Molina, J. Bonastre, F. Cases, Influence of electrochemical reduction and oxidation processes on the decolourization and degradation of C.I. Reactive Orange 4 solutions. Chemosphere 75 (2009) 1329-1337.
<http://dx.doi.org/10.1016/j.chemosphere.2009.02.063>
- [22] A.I. del Río, M. Benimeli, J. Molina, J. Bonastre, F. Cases, Electrochemical treatment of C.I. Reactive Black 5 solutions on stabilized doped Ti/SnO₂ electrodes. International Journal of Electrochemical Science 7 (2012) 13074-13092.
- [23] F. Vicent, E. Morallón, C. Quijada, J.L. Vázquez, A. Aldaz, F. Cases, Characterization and stability of doped SnO₂ anodes. Journal of Applied Electrochemistry 28(6) (1998) 607-612.
<http://dx.doi.org/10.1023/A:1003250118996>
- [24] R. M. Christie, *Colour Chemistry. 2nd edition.* Ed. Royal Society of Chemistry. 2012.
- [25] K. Lacasse, W. Baumann, Textile Chemical. Environmental data and facts. Ed. Springer-Verlag. 2004
- [26] A.I. del Río, J. Fernández, J. Molina, J. Bonastre, F. Cases, Electrochemical treatment of a synthetic wastewater containing a sulphonated azo dye. Determination of naphthalenesulphonic compounds produced as main by-products. Desalination. 273 (2011) 428-435.
<http://dx.doi.org/10.1016/j.desal.2011.01.070>

- [27] E.W. Rice, R.B. Baird, A.D. Eaton, L.S. Clesceri, Standard Methods for the Examination of Water and Wastewater. 22nd Ed. APHA/American Water Works Association/Water Environment Federation. USA. 2012.
- [28] L. Bilińska, M. Gmurek, S. Ledakowicz, Comparison between industrial and simulated textile wastewater treatment by AOPs – Biodegradability, toxicity and cost assessment. Chemical Engineering Journal 306 (2016) 550-559.
<http://doi.org/10.1016/j.cej.2016.07.100>
- [29] W. Stumm, J.J. Morgan, Aquatic Chemistry: Chemical Equilibria and Rates in Natural Waters, 3rd Ed. John Wiley & Sons, 1995
- [30] Ch. Comninellis, C. Pulgarin, Anodic oxidation of phenol for wastewater treatment. Journal of Applied Electrochemistry 21 (1991) 703-708.
<http://dx.doi.org/10.1007/BF01034049>
- [31] P. Li, W. Cai, Y. Xiao, Y. Wang, J. Fan, Electrochemical degradation of phenol wastewater by Sn-Sb-Ce modified granular activated carbón. International Journal of Electrochemical Science 12 (2017) 2777-2790.
<http://doi.org/10.20964/2017.04.58>
- [32] A. Kapalka, G. Fóti, Ch. Comninellis, Electrochemistry for the Environment. 1st Ed. Springer, New York 2010.
- [33] N. Jarrah, N.D. Mu'Azu, Simultaneous electro-oxidation of phenol, CN⁻, S²⁻ and NH₄⁺ in synthetic wastewater using boron doped diamond anode. Journal of Environmental Chemical Engineering 4(2016) 2656-2664.
<http://doi.org/10.1016/j.jece.2016.04.011>
- [34] H. Akroud, L. Bousselmi, Chloride ions as an agent promoting the oxidation of synthetic dyestuff on BDD electrode. Desalination and Water Treatment 46 (2012) 171-181.
<http://doi.org/10.1080/19443994.2012.677528>
- [35] H.-Y. Li, J. Gao, Y.-Z. Liu, Electrochemical reaction for phenol on Ti/IrO₂-Ta₂O₅ electrode. Hanneng Cailiao/Chinese Journal of Energetic Materials 24 (2016) 289-294.
<http://doi.org/10.11943/j.issn.1006-9941.2016.03.014>
- [36] M. Xu, Z. Wang, F. Wang, P. Hong, C. Wang, X. Ouyang, C. Zhu, Y. Wei, Y. Hun, W. Fang, Fabrication of cerium doped Ti/nanoTiO₂/PbO₂ electrode with improved electrocatalytic activity and its application in organic degradation. Electrochimica Acta 201 (2016) 240-250.
<http://doi.org/10.1016/j.electacta.2016.03.168>
- [37] J.R. Bolton, K.G. Bircher, W. Tumas, C.A. Tolman, Figures-of-merit for the technical development and application of advanced oxidation technologies for

both electric- and solar-driven systems (IUPAC Technical Report). Pure Applied Chemistry 73 (2001) 627 – 637.
<http://dx.doi.org/10.1351/pac200173040627>.

- [38] R.M. Silverstein, F.X. Webster, D.J. Kiemle, D.L. Bryce, Spectrometric Identification of Organic Compounds. 8th Ed. John Wiley & Sons, 2015.
- [39] J. Yang, Analysis of Dye. Chemical Industry Press, Beijing Ed, 1987.
- [40] W. Feng, D. Nansheng, H. Helin, Degradation mechanism of azo dye C. I. reactive red 2 by iron powder reduction and photooxidation in aqueous solutions. Chemosphere 41 (2000) 1233–1238.
[http://dx.doi.org/10.1016/S0045-6535\(99\)00538-X](http://dx.doi.org/10.1016/S0045-6535(99)00538-X)
- [41] C. Galindo, P. Jacques, A. Kalt, Photodegradation of the aminoazobenzene acid orange 52 by three advanced oxidation processes: UV/H₂O₂, UV/TiO₂ and VIS/TiO₂: Comparative mechanistic and kinetic investigations. Journal of Photochemistry and Photobiology A: Chemistry 130 (1) (2000) 35–47.
[http://dx.doi.org/10.1016/S1010-6030\(99\)00199-9](http://dx.doi.org/10.1016/S1010-6030(99)00199-9)
- [42] M. Styliidi, D.I. Kondarides, X.E. Verykios, Visible light-induced photocatalytic degradation of Acid Orange 7 in aqueous TiO₂ suspensions. Applied Catalysis B: Environmental 47 (2004) 189–201.
<http://dx.doi.org/10.1016/j.apcatb.2003.09.014>
- [43] P.A. Carneiro, C.S. Fugivara, R.F.P. Nogueira, N. Boralle, M.V.B. Zanoni, A Comparative study on chemical and electrochemical degradation of Reactive Blue 4 dye. Portugalae Electrochimica Acta 21 (2003) 49-67.
- [44] G. Socrates, Infrared Characteristic Group Frequencies. 3rd ed., John Wiley & Sons, New York, 1997.
- [45] M. Snehalatha, C. Ravikumar, N. Sekar, S.V. Jayakumar, H. Joe, FT-Raman, IR and UV-visible spectral investigations and ab initio computations of a nonlinear food dye amaranth. Journal of Raman Spectroscopy 39 (2008) 928–936.
<http://dx.doi.org/10.1002/jrs.1938>

HIGHLIGHTS

- Electrolyses of real dyestuff wastewater of a complex mix of reactive dyes are made.
- Enhanced stability Ti/SnO₂–Sb–Pt anodes permit complete decolorisation.
- Noticeable mineralization of organic matter is obtained without chloride addition.
- The purpose treatment is a valuable alternative for textile wastewater remediation.

GRAPHICAL ABSTRACT



TABLE CAPTIONS

Table 1: Review of different electrochemical processes for the electrochemical treatment of wastewater from textile dyeing.

Table 2: Description of the selected reactive dyes.

Table 3: Kinetics analyses and energy consumption obtained for all the electrolyses: decolourization kinetics rate ($A^{-1} h^{-1} L$), specific charge ($A \text{ hL}^{-1}$) for a complete decolourization (99 per cent) and energy consumption ($kWh L^{-1}$).

Table 4: Results of TOC removal, COD removal, values of AOS, COS and ACE of samples obtained at different loaded charges in the electrolysis processes.

FIGURE CAPTIONS

Figure 1: Molecular structure of the three dyes of the HEXL Trichromy.

Figure 2: Undivided filter press reactor

Figure 3: Evolution of the chromatographic profile during the electrolysis of the solutions of: a) Procion Yellow®, b) Procion Crimson® and c) Procion Navy®. d) Logarithm of the normalised chromatographic area versus loaded charge Q (Ah L^{-1}) of samples obtained during the redox process at 125 mA cm^{-2} . The initial solutions were the three hydrolysed dyes obtained after the dyeing processes.

Figure 4: Evolution of the UV-Vis spectra of the trichromy solution with the loaded charge during the electrolysis. The bands related with the three chromophores are centered at 420 nm, 549 nm and 610 nm, approximately.

Figure 5: FTIR spectra of the trichromy solution before and after electrolysis.

Table 1

Dye/Concentration	Electrolyte	Anode	Molecular structure	Removal	Reference
Reactive Black 5/ 20 mg L⁻¹	HCl pH 4	TiO ₂ -Graphene oxide	Simple	80% decolouration	[3]
4-amino-3-hydroxy-2-p-tolylazo-naphthalene-1-sulfonic Acid/ 175 mg L ⁻¹	0.05 M Na ₂ SO ₄	Boron-doped diamond	Simple	92% TOC	[4]
Reactive Black 5/ 20 mg L⁻¹	2 10 ⁻⁵ M Na ₂ SO ₄	Boron-doped diamond	Simple	82% TOC	[5]
Remazol Red/ 100 mg L ⁻¹	0.3-5.0 g L ⁻¹ NaCl	Anaerobic biofilm	Medium	> 90% COD	[6]
Reactive Blue 19/ 100 mg L ⁻¹	Potato dextrose at pH 6.8	Chemical oxidation by Endophytes	Medium-simple	90% decolouration	[7]
Reactive Yellow 160/ 100 mg L ⁻¹	4 g L ⁻¹ NaCl	PbO ₂ , SnO ₂	Simple	100% COD	[12]
Alphazurine/ 500 mg L ⁻¹	0.5 M Na ₂ SO ₄	PbO ₂	Simple	90% COD	[12]
Methyl Red/ 100 mg L ⁻¹	H ₂ SO ₄ pH 3	PbO ₂	Simple	90% COD	[12]
Reactive Orange 16/ 85 mg L ⁻¹	0.1 M Na ₂ SO ₄	β-PbO ₂	Simple	90% TOC	[12]
Methyl Green/ 300 mg L ⁻¹	0.5 M H ₂ SO ₄	PbO ₂	Simple	82% TOC	[12]
Mixture of real dyeing textile effluents	170 mg L ⁻¹ Cl ⁻ + 19 mg L ⁻¹ SO ₄ ²⁻	Boron-doped diamond	Unknown	90% COD	[17]

Table 2

Abbr	Comercial Name	C.I. Name	Chromophore	Reactive group	λ_{max} (nm)
PY	Procion Yellow HEXL	Reactive Yellow 138:1	Diazo	Monoclorotriazinic	420
PC	Procion Crimson HEXL	Reactive Red 231	Diazo	Monoclorotriazinic	549
PN	Procion Navy HEXL	Non registered	Diazo	Monoclorotriazinic	610

Table 3

DYE SOLUTION	λ (nm)	Kap (A ⁻¹ h ⁻¹ L)	Qdec (Ah L ⁻¹)	EEO (kWh m ⁻³)
PROCION YELLOW HEXL	420	0.076	62.18	32.18
PROCION CRIMSON HEXL	549	0.054	88.40	106.30
PROCION NAVY HEXL	610	0.061	75.81	91.60

Table 4

DYE SOLUTION	Q (A.h L ⁻¹)	TOC (mgL ⁻¹)	TOC REMOVAL (%)	COD (mg L ⁻¹)	COD REMOVAL (%)	AOS	ΔAOS	COS	ΔCOS	ACE (%)
P. YELLOW	0.00	271.55	-	882.67	-	-0.88	-	-0.88	-	-
	89.71	232.50	14.38	648.00	26.59	-0.18	0.70	-0.15	0.72	1.11
	239.41	170.25	37.30	520.00	41.09	-0.58	0.29	-0.36	0.51	0.70
P. CRIMSON	0.00	422.00	-	1768.00	-	-2.28	-	-2.28	-	-
	89.71	388.35	7.97	1319.33	25.38	-1.10	1.19	-1.01	1.28	2.12
	218.78	338.80	19.72	986.00	44.23	-0.37	1.92	-0.29	1.99	1.63
P. NAVY	0.00	351.45	-	1312.00	-	-1.60	-	-1.60	-	-
	92.42	293.65	16.45	826.00	37.04	-0.22	1.38	-0.18	1.42	2.24
	244.00	206.20	41.33	533.33	59.35	0.12	1.72	0.07	1.67	1.50
TRICHRAMY	0.00	346.35	-	1192.00	-	-1.16	-	-1.16	-	-
	92.42	330.10	4.69	896.50	24.79	-0.07	1.09	-0.07	1.09	1.36
	247.39	252.70	27.04	682.67	42.73	-0.05	1.11	-0.04	1.12	0.97

Figure 1

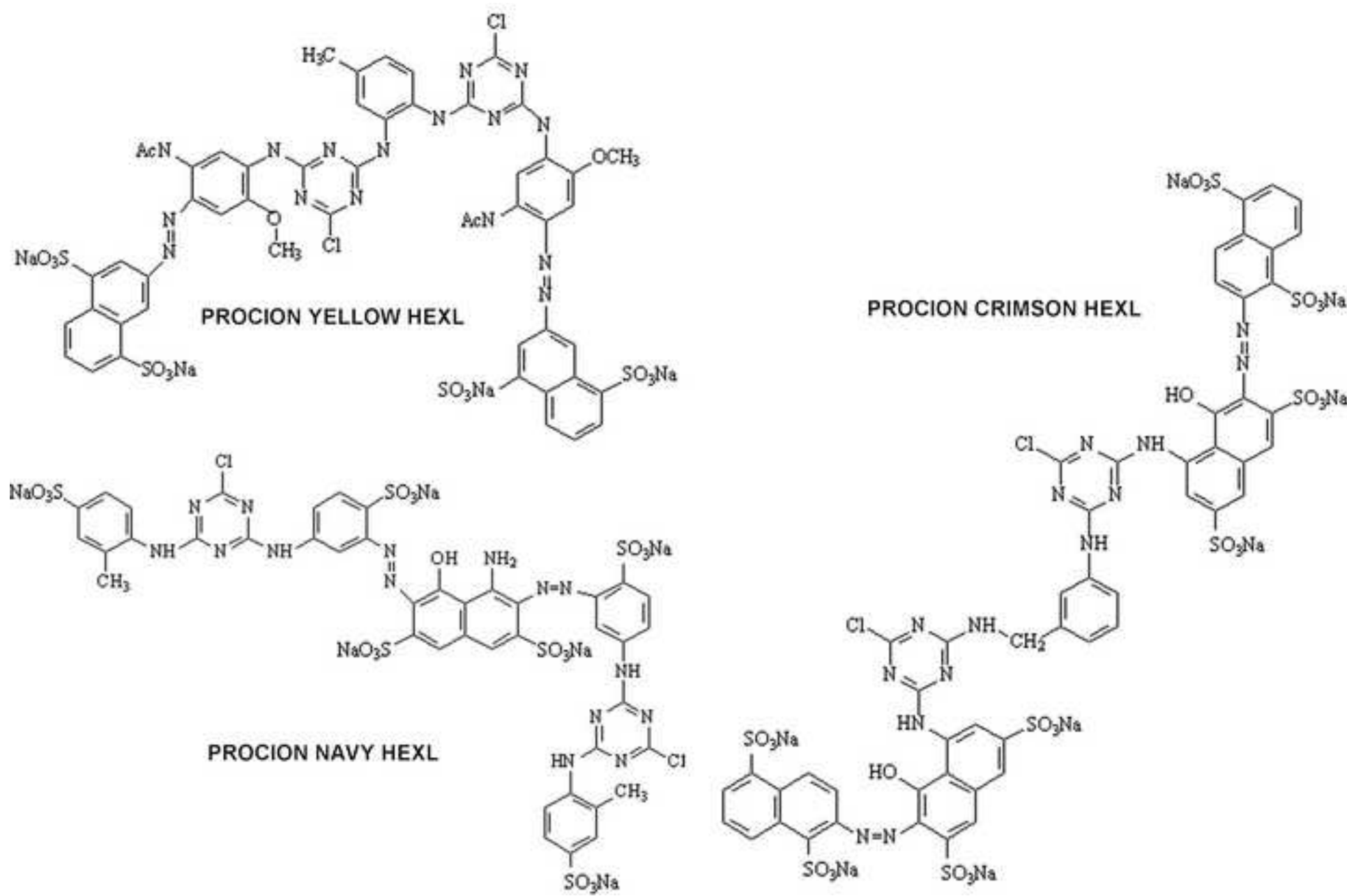
[Click here to download high resolution image](#)

Figure 2

[Click here to download high resolution image](#)

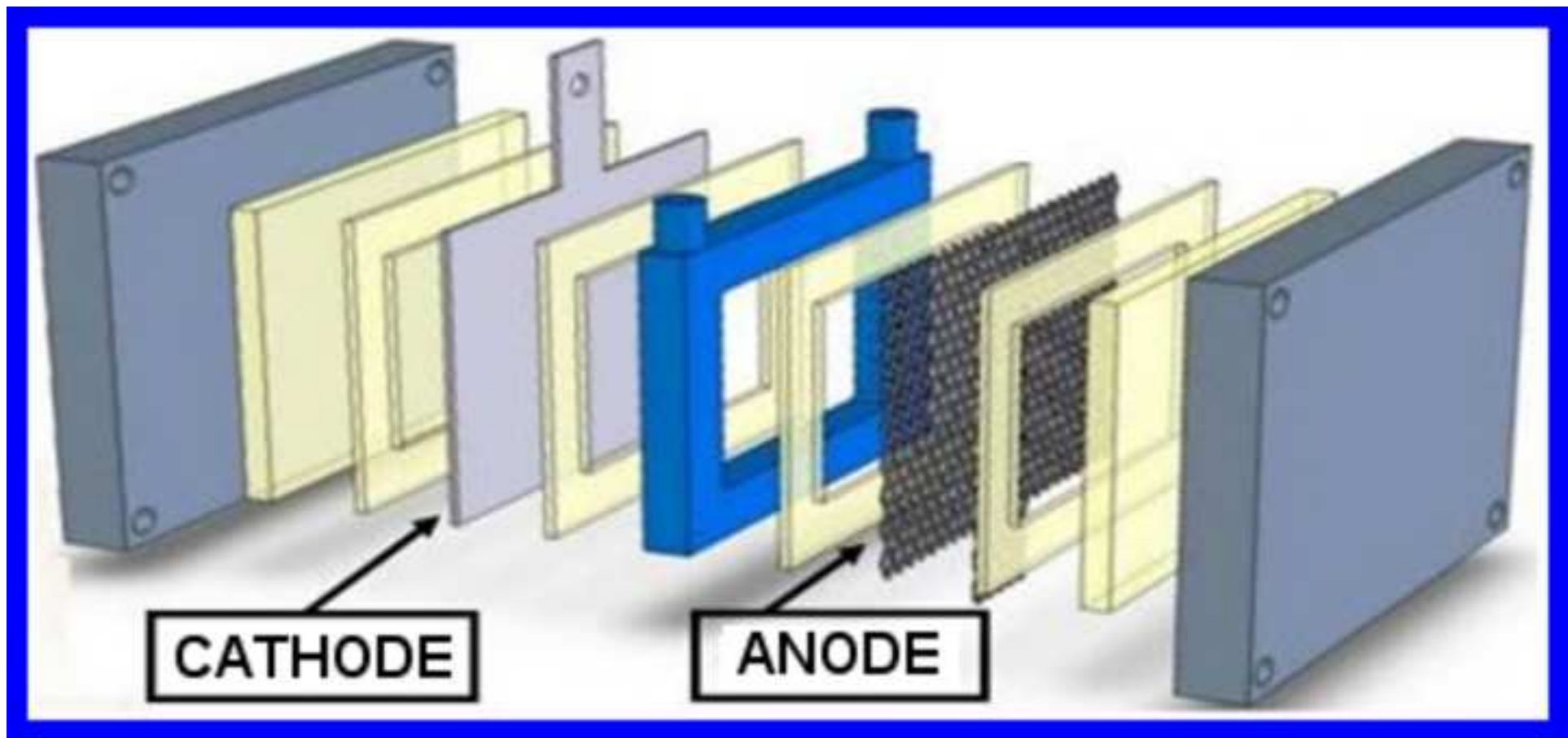


Figure 3

[Click here to download high resolution image](#)

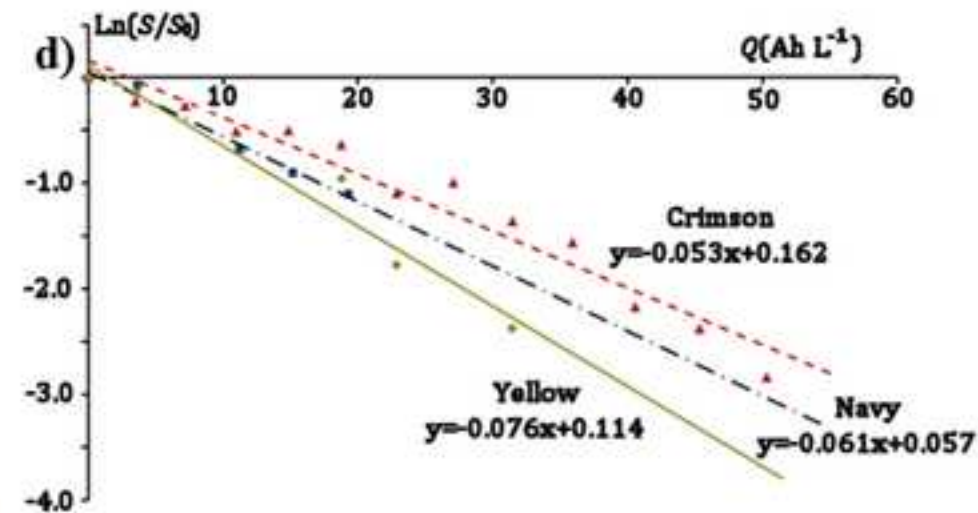
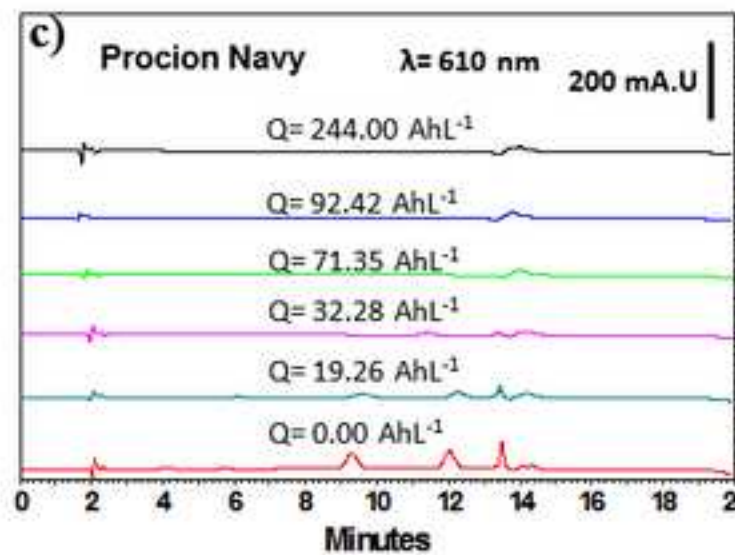
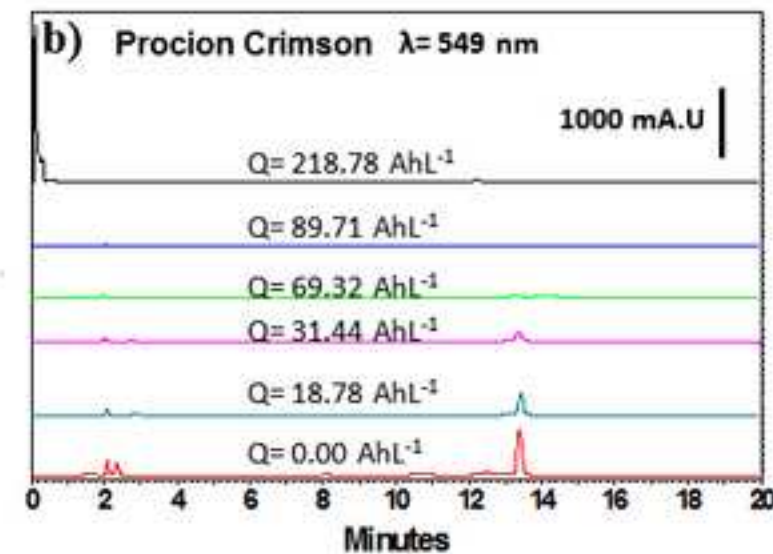
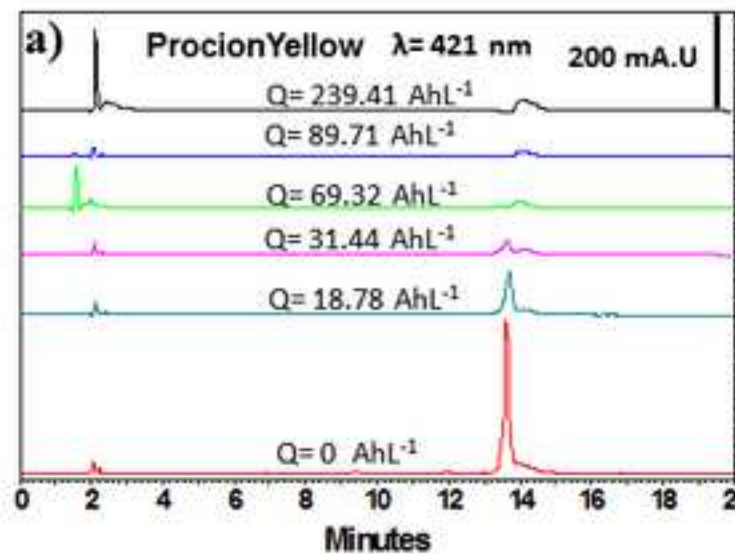


Figure 4

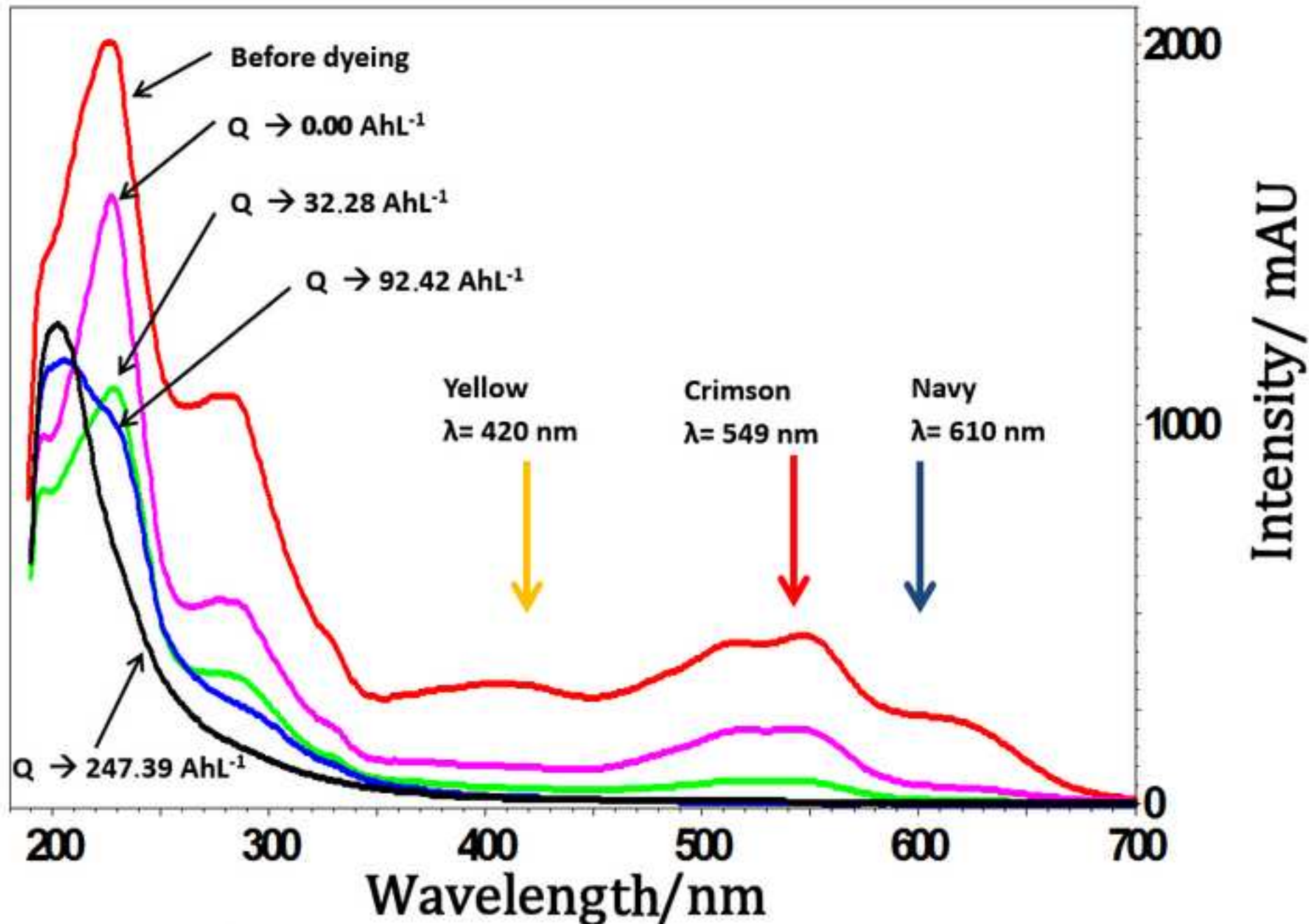
[Click here to download high resolution image](#)

Figure 5

[Click here to download high resolution image](#)

